J Solid State Electrochem (2007) 11:138–143
DOI 10.1007/s10008-006-0212-1

ORIGINAL PAPER

Influence of bath composition and deposition parameters on nanostructure and thermal stability of gold

O. Yevtushenko · H. Natter · R. Hempelmann

Received: 27 October 2005 / Revised: 1 March 2006 / Accepted: 30 March 2006 / Published online: 11 October 2006

Abstract Nanocrystalline gold is electrodeposited from a stable nontoxic bath, in which Au^{+} is stabilized by complex formation with 3-mercapto-1-propanesulfonic acid sodium salt. Nanoscaling is achieved by pulse techniques. The crystallite size is strongly dependent on physical and chemical process parameters, such as pulse duration, current density, bath temperature, type, and amount of additives; especially, we observe a decrease of the crystallite size down to 16 nm by the proper choice of current density and temperature, and down to 7 nm by the use of additives. The thermal stability of nanocrystalline gold is investigated by in situ high-temperature X-ray diffraction; nanogold exhibits a thermal stability up to 673 K. An activation energy of 37 kJ mol^{-1} is determined for the grain-growth kinetics.

Keywords Nanostructured gold · Pulsed electrodeposition · Thermal stability

Introduction

The preparation of nanostructured materials by electroplating has received much attention in the last decades because of the possibility to control the physical and chemical properties of the deposits by tuning of the crystallite size [1–4].

Gold is important in electronic devices for electrical contacts and for bonding [5, 6]; with further miniaturization of the electronic structures on integrated circuits, also the diameter of the bond wires has to decrease. For future wire diameters below 1 μm, the grain size must be below 100 nm in order to avoid a bamboo-like microstructure with grain boundaries extending over the whole diameter and with correspondingly low mechanical stability. For those reasons, the improvement in mechanical properties of gold, as brought about by nanoscaling, is highly welcome. Generally, with decreasing crystallite size, a metal becomes harder [1–4]. Simultaneously, sufficient thermal stability must be assured: If grain growth takes place during operation, i.e., at the operation temperature of the device, the mechanical properties deteriorate.

For many decades, cyanide-containing baths for gold and gold alloy electrodeposition were used. On the one hand, the $Au(CN)_2$ and $Au(CN)_4$ complexes are very stable, cyanide salts are very cheap, and the gold preparation process is well known [7]. On the other hand, cyanide is very poisonous even at a very low concentration. A number of attempts to produce gold electrolytes from thiomalate, mercaptoethanol, iodide, hydroxide, thiosulfate, sulfite, tetraaminonitrate, and phosphoric acid were made [3, 8, 9]. The disadvantages of these electrolytes are instability, toxicity, and water sensitivity [10]. We report here about a stable and nontoxic electrolyte for gold electrodeposition using a 3-mercapto-1-propanesulfonic acid sodium salt (MPS) as complexing agent.

The following contribution describes the synthesis of this nontoxic electrolyte for the electrodeposition of nanostructured gold and gold alloys. We also investigate

Paper presented at the "Jahrestagung der Fachgruppe Angewandte Electrochemie der Gesellschaft Deutscher Chemiker, Düsseldorf, 11.–14.06.2005"

O. Yevtushenko · H. Natter · R. Hempelmann (✉)
Universität des Saarlandes, Physikalische Chemie,
66123 Saarbrücken, Germany
e-mail: r.hempelmann@mx.uni-saarland.de

the influence of the deposition parameters and the bath composition on the crystallite size and thermal stability.

Theoretical background

The pulsed electrodeposition (PED) technique is a versatile method for the preparation of nanostructured metals and alloys [11, 12]. The formation of nanostructured materials by electrodeposition comprises the nearly instantaneous formation of a large number of nuclei and the comparatively slow growth of the deposited nuclei. The control of both processes is possible by the variation of pulse parameters (I_P, average current density; t_{on}, duration of pulses; t_{off}, duration between two pulses), by the variation of the bath temperature, and by the electrolyte composition (e.g., additives, grain refiners, brighteners).

According to the theory of nucleation [13], the size and number of nuclei depend on the overvoltage η:

$$r = \frac{2\sigma V}{ze_0|\eta|} \quad (1)$$

In this electrochemical version of the Kelvin equation, r means the critical nucleation radius, σ the specific surface energy, V the atomic volume in the crystal, and z the number of elementary charges e_0. A high-nucleation density on the electrode surface can be achieved by a high overvoltage. This high overvoltage can only be maintained for a few milliseconds because the metal ion concentration in the vicinity of the cathode decreases, and therefore, the process would become diffusion-controlled [14]. During the t_{off} time, the metal ions diffuse from the bulk electrolyte to the cathode and compensate the metal ion depletion. Also during the t_{off} time, due to exchange current processes, Ostwald ripening sets in, which means that the larger crystallites, which are energetically more preferred, grow at the expense of the smaller crystallites. This process can be impeded by surface active substances (grain refiners) as additives to the electrolyte.

Experimental

The bath is prepared using commercial tetrachloroaurate (III) acid from ChemPur (Au%; 50.0), MPS (tech., 90%) from Aldrich, and 50% ammonium hydroxide solution.

For pulsed electrodeposition under galvanostatic conditions, a cell with an anode consisting of high acid-resistant stainless steel of low iron content (V4A) and a copper cathode (99.99% purity) is used. For every experiment, the cathode is polished with emery silicon carbide paper (8–4 μm grain size), thoroughly cleaned in sulfuric acid (95–97%), and rinsed with distilled water. Copper, as cathode material, was used because it is isostructural with gold with a nearly identical lattice content, which avoids surface cracks and minimizes microstrain in the deposit [14]. Surface cracks and a high level of microstrain in the gold deposit have been observed when using a glassy carbon cathode. For alloy deposition, platinum(II) nitrate (Pt%; 59.0) from ChemPur, palladium (II) chloride (Pd%; 60.0) from Fluka, silver nitrate (Ag%; 99.8) from Merck, and cupric sulfate pentahydrate (Cu%; 99.0) from Fluka are used.

The polarization measurements are carried out using a potentiostat EG&G Instruments Model 6310 in standard three electrodes cell. We use a platinum counter electrode and $Hg/HgSO_4$ reference electrode (the presented potentials are quoted in the present contribution, however, with respect to the normal hydrogen electrode). The linear sweep voltammograms (LSV) are recorded with a scan rate of 100 mV/s at room temperature.

All X-ray diffraction (XRD) measurements are performed using a Siemens D-5000 diffractometer calibrated with a LaB_6-standard sample. The diffractometer is equipped with a position-sensitive detector, which allows recording the scattering intensity over a 2θ range of 15°.

Transmission electron microscopy and XRD are used for the determination of crystallite sizes, with line-width and line-shape evaluation according to Scherrer and Warren and Averbach [15–17], respectively. All details of the latter procedure, appropriately modified for routine measurements, have been described elsewhere [18, 19].

Energy dispersive X-ray (EDX) analysis is used for the elementary analysis of the deposits.

Results and discussion

Preparation of the electrolyte

The electrolyte for gold electrodeposition is prepared according to the following reactions:

$$H[AuCl_4] \xrightarrow{Base} Au(OH)_3$$
$$Au(OH)_3 + 4HS - R \rightarrow \left[Au(S-R)_4\right]^- + 3H_2O + H^+$$
$$\left[Au(S-R)_4\right]^- \xrightarrow{time\ or\ \Delta T} \left[Au(S-R)_2\right]^- + R - S - S - R$$

where R presents $-(CH_2)_3-SO_3Na$ and $HS-(CH_2)_3-SO_3Na$; 3-mercapto-1-propanesulfonic acid sodium salt is henceforth abbreviated as MPS.

The reaction of tetrachlorogold-(III) acid with ammonium hydroxide leads to gold-(III) hydroxide, which reduces to the gold (I)–thiol-containing complex by interacting with MPS [20]. The resulting solution is colorless and exhibits long time stability. The electrolyte consists of 5 g l^{-1}

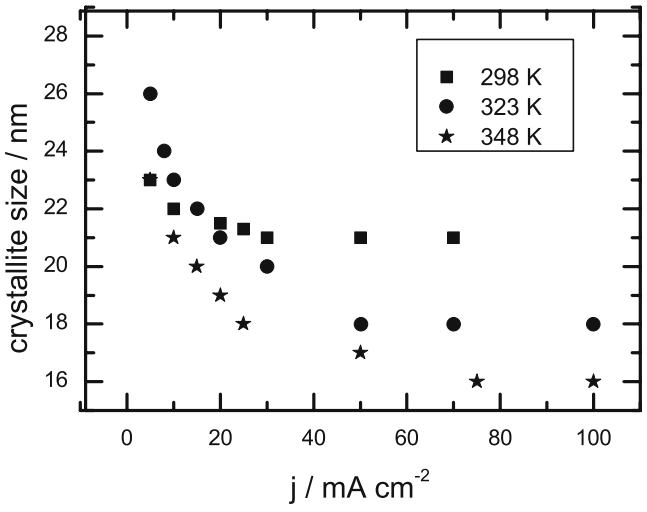

Fig. 1 Dependence of the crystallite size on the bath temperature and the average current density. It is evident from the picture that the crystallite size of gold decreases with increasing the temperature of the bath and with increasing current density. Pulse duration t_{on}=1 ms, duration between two pulses t_{off}=20 ms

$H[AuCl_4]$, 10.5 g l^{-1} MPS, and 160 ml (50%) NH_4OH. The pH was adjusted to 10.

Pulsed electrodeposition

All PED experiments are made with the following pulse parameters: t_{on}=1 ms and t_{off}=20 ms. The dependence of the crystallite size on the bath temperature and current density is investigated (see Fig. 1), changing the bath temperature from 298 to 348 K and the current density from 10 to 100 mA cm^{-2}. The crystallite size decreases both with increasing bath temperature and with increasing current density (see Fig. 1). Upon a temperature change from 298 to 348 K, the crystallite size changes from 28 to 16 nm, whereas an increase of the current density from 5 to 100 mA cm^{-2} causes a decrease in crystallite size by a factor of 1.5. This behavior is also reported by Lin and Weil [21]. The sulfur atoms act as grain refiner by covering the fresh deposited gold nuclei and prevent further crystallite growth, probably by interaction of the free electron pairs of the sulfur atoms with the metal surface [8]. In support of this assumption, the EDX analysis shows the presence of sulfur in the deposited gold samples.

The influence of the organic and inorganic grain refiners on the nanostructure of gold is investigated. As standard organic additives, we have chosen tartaric acid (c=0.5 g l^{-1}), benzoic acid (c=0.5 g l^{-1}), nicotinic acid (c=0.5 g l^{-1}), and Na-saccharin (c=2.5 g l^{-1}), but none of them brought about the expected result. As shown in Table 1, instead of a decrease of the crystallite size, the reverse effect is observed: The crystallite size increases with increasing current density. A possible explanation of this behavior could be that the free electron pairs of the additives react with thiol species in the electrolyte, which leads to a release of gold ions. This accelerates the Ostwald ripening and causes the growth of larger gold crystallites.

As inorganic additive $NaAsO_2$ is added in an amount of 0.5 g l^{-1}: Just this small amount decreases the crystallite size down to 10 nm. Probably, the nanocrystals in this way are protected against Ostwald ripening by the adsorption of the arsenic compound. It was also shown by Dinan and Cheh [4] that arsenic additives in a phosphate bath for gold electrodeposition decrease the crystallite size and therefore increase the hardness of the deposits.

The serial cathodic LSV measurements are made in an additive-free electrolyte and in a bath with additives. The polarization curves are recorded at 100 mV/s between E=0.6 V and E=−1.5 V in the negative cathodic direction, where the gold electrodeposition occurs (see Fig. 2). To initiate the deposition of gold atoms on the surface of the electrode, a sufficiently negative potential is required. If the surface of the cathode is partially blocked by sulfur- or arsenic-containing substances, the deposition becomes more difficult and therefore a larger overpotential is needed. A change of the minimum potential required for gold deposition is observed depending on the type of additives. In Fig. 2, it is shown that the arsenic-containing electrolyte causes the largest potential, whereas the nicotinic acid-

Table 1 Dependence of the crystallite size on the current density in the presence of different additives (benzoic acid, sodium saccharin, nicotinic acid, tartaric acid, $NaAsO_2$) at room temperature

I_p (mA cm^{-2})	Crystallite size (nm)					
	Additive-free	Benzoic acid	Na saccharin	Nicotinic acid	Tartaric acid	$NaAsO_2$
10	28	22	25	23	25	10
30	22	26	28	28	27	10
50	21	28	30	31	30	8
100	21	37	39	37	35	7

The concentrations are given in the text. The experimental uncertainty in the crystallite size is between 3 and 7 nm, depending on the size.

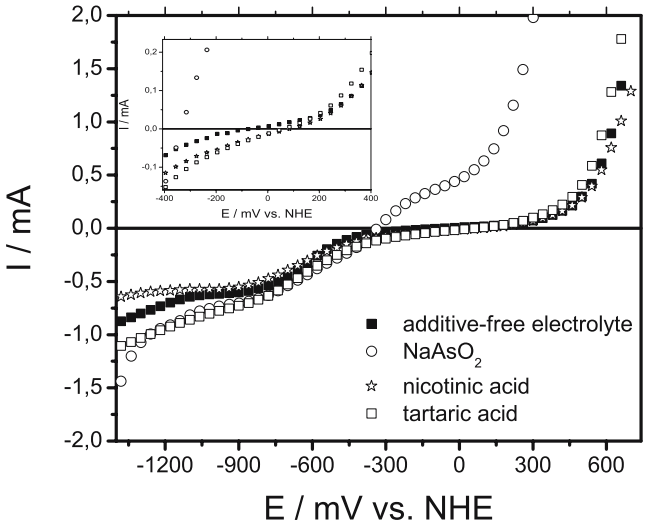

Fig. 2 LSV measurements. Influence of different additives on the potential required for the cathodic reaction [*filled squares*, additive-free; *empty circles*, $NaAsO_2$ (c=0.5 g l^{-1}); *empty stars*, nicotinic acid (c=0.5 g l^{-1}); *empty squares*, tartaric acid (c=0.5 g l^{-1})]. The measurements start at positive potentials and move into negative direction where gold deposition occurs. The *inset* enlarges the measurements in the potential range [+250; −400] mV

containing bath the smallest, even smaller than the additive-free electrolyte. As was mentioned above, nicotinic acid and tartaric acid react with the gold–thiol complex; some gold ions become free, and, therefore, a less negative potential is required for the cathodic reaction.

We investigate the effectiveness of the pure electrolyte with the following pulse parameters: t_{on}=1 ms, t_{off}=20 ms, and I_P of 50 mA cm^{-2} at room temperature. The total amount of gold in the electrolyte was 68 mg. During the first hour of PED, we observed a rapid increase of the deposition rate: in 10, 20, and 40 min, 10, 18, and 30 mg of gold metal are deposited, respectively. This rate decreased during the next 2 h; no change in the deposition rate is observed, and the total mass of the deposited nanocrystalline gold is 40 mg. The effectiveness of the electrolyte at room temperature is 70%. During the (galvanostatically operated) experiment, the voltage between the cathode and the anode was measured, which eventually increased to −3.2 V. This magnitude is high enough to initiate a side reaction—hydrogen evolution. Hydrogen evolution on the cathode could possibly decrease the current efficiency, and probably for this reason, the effectiveness of the electrolyte reaches only 70%. The bath exhibits long-time stability (some months). All deposited samples have smooth and shining surfaces.

Nanoscaled gold alloys with silver, palladium, copper, and platinum are deposited with I_P=50 mA cm^{-2}, t_{on}=1 ms, and t_{off}=20 ms at room temperature. The alloy composition can be controlled by the metal ion concentration in the bath.

Table 2 Bath compositions for gold alloy deposition and the resulting crystallite sizes

Metal salts	Concentration (g l^{-1})	Crystallite size (nm)	Au content in alloy (%)
$AgNO_3$	3.75	30	34
$AgNO_3$	2.5	35	79
$AgNO_3$	3.35	28	89
$PdCl_2$	0.7	12	70
$NaAsO_2$	0.5		
$PdCl_2$	0.5	9	88
$NaAsO_2$	0.5		
$Pt(NO_3)_2$	1.5	28	67
$Pt(NO_3)_2$	0.5	30	86
$CuSO_4{\cdot}5H_2O$	0.5	20	71
$CuSO_4{\cdot}5H_2O$	1.5	28	92

It is shown that by changing the concentrations of chemicals in the electrolyte, binary alloys with different Me contents and crystallit sizes are deposited. Deposition conditions: I_p=50 mA cm^{-2}, t_{on}=1 ms, t_{off}=20 ms, room temperature. The experimental uncertainty in the crystallite size is between 4 and 6 nm, depending on the size.

As metal source, we use $AgNO_3$, $PdCl_2$, $CuSO_4{\cdot}5H_2O$, and $Pt(NO_3)_2$ in different amounts (see Table 2). The alloy composition of the resulting deposits was calculated from the respective lattice constants, which are determined by XRD. The results are compared with the literature data and

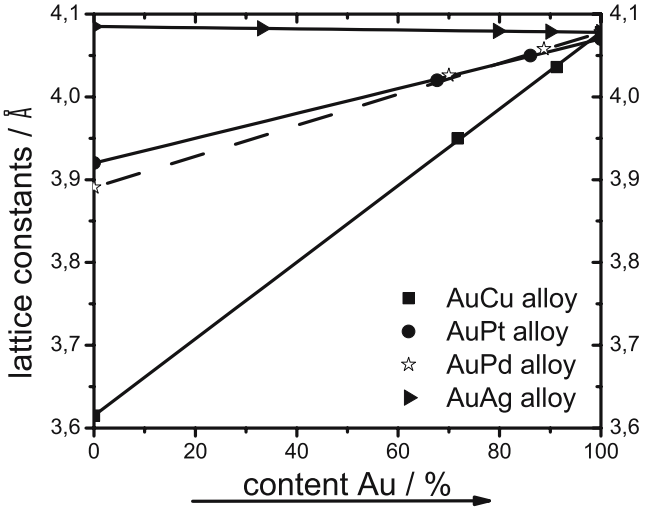

Fig. 3 Determination of the composition of binary gold alloys by X-ray diffraction. On the *left-hand ordinate axis*, the lattice constants for pure silver, platinum, palladium, and copper metals are given (from *top to bottom*), respectively. On the *right-hand ordinate axis*, the lattice constant for pure gold is displayed. From a comparison of the measured lattice constants of the alloys with the linear interpolations (*straight lines* in the figure), the binary alloys' composition has been determined. The experimental uncertainty in the lattice constants is below ±0.05 Å

show a good agreement [22]. The metal percentage in the deposit is determined from a calibration curve "lattice constant versus the gold content" (see Fig. 3).

High-temperature XRD measurements

The stability of the electrodeposited gold nanocrystallites at high-temperature conditions is investigated with XRD using a position-sensitive detector (Braun Inc., Germany). In the angular range $35° \leq 2\theta \leq 50°$ covered by the detector, we observe the gold (111) and (200) Bragg reflections. The samples deposited from the additive-free MPS bath (sample 1) and from the bath containing $NaAsO_2$ (sample 2) are heated in air from 298 to 1,073 K with a rate of 2 K/min (scan duration, 5 min). Every 5 min, a new diffractogram is recorded during the temperature ramp. The crystallite sizes resulting from the widths are shown in Fig. 4. Figure 4 shows that samples 1 and 2 do not exhibit any grain growth up to 623 K. This indicates a higher thermal stability than samples deposited from a sulfite bath: Cojocaru et al. [23] have observed a thermal stability only up to 323 K, whereas we previously [3] have observed a thermal stability of gold samples deposited from sulfite baths up to 423 K. Obviously, our present gold samples have such a high-thermal stability because of the presence of sulfur or arsenic atoms in the grain boundaries. Very likely, the first plateau (see Fig. 4) is caused by these impurities segregated in the grain boundaries. These results are in a good accordance with Carotenuto and Nicolais [24]: They concluded that the thermal stability (up to ca. 573 K) of thiol-derivatized gold clusters results from strong bonds of the thiol group with the metal surface. To prove the assumption of the influence of sulfur compound on the thermal stability of gold nanocrystals, the concentration of MPS was doubled (sample 3). The sample was deposited under the same conditions. As expected, sample 3 shows a better thermal stability (up to 673 K) than samples 1 and 2 (see Fig. 4). Above 673 K, a fast crystallite growth up to 32 nm (sample 1), up to 25 nm (sample 2), and up to 27 nm (sample 3) is observed. Apparently, the fast growth is caused by the decomposition of the –SH bonds, which takes place at this temperature. As expected, the different content of sulfur or arsenic in the deposit leads to different crystallite sizes.

According to the EDX analysis, the content of sulfur atoms decreases during the heating process. From the high-temperature experiments, we conclude that sulfur- or arsenic-containing additives decrease the gold crystallite size during the electroplating process by segregating in the grain boundaries, and therefore increase the thermal stability of deposited gold.

For the determination of kinetic data, like the activation energy for the crystallite growth of nanostructured gold, we performed isothermal XRD growth experiments at 573, 623, 673, and 723 K. The experimental data were evaluated with a kinetic model with size-dependent impediment where, according to Michels et al. [25], the retarding term should be a function of the grain size in the grain-growth process of nanocrystalline metals [19]. Figure 5 shows the comparison between measured data and least-square fits of the model. The temperature dependence of the rate

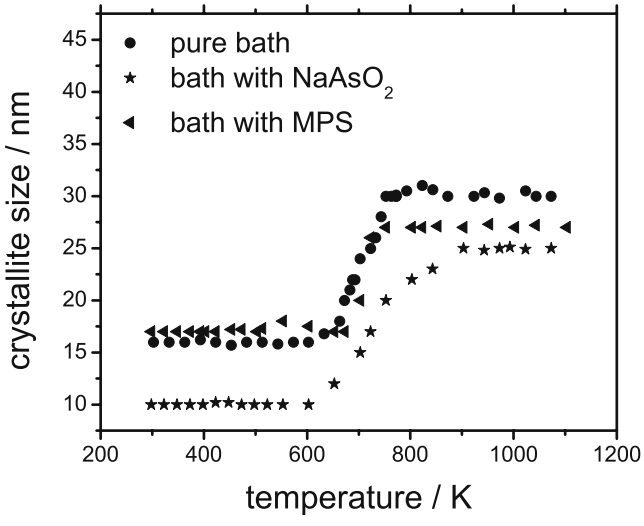

Fig. 4 Measurement of the thermal stability of nanostructured gold. *Filled circles*, *filled stars*, and *filled triangles* represent the heating results for samples deposited from the additive-free MPS electrolyte, a bath with $NaAsO_2$ (c=0.5 g l^{-1}), and a bath with additional MPS as additive (c=10 g l^{-1}), respectively. The experimental uncertainties in the sizes did not exceed 5 nm

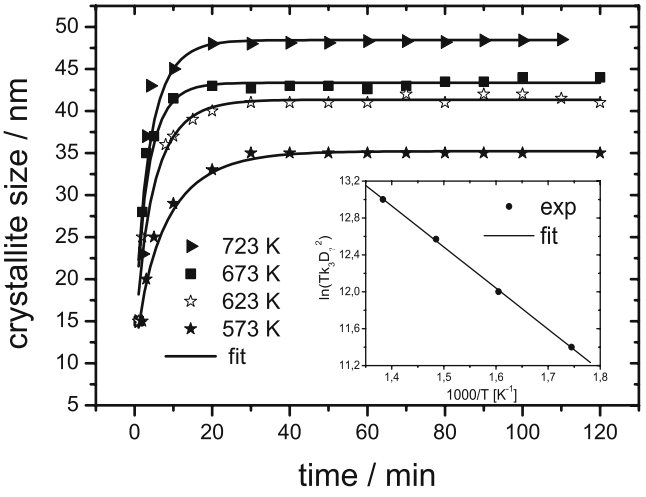

Fig. 5 Grain-growth isotherms of nanostructured gold deposited from the additive-free MPS bath (I_P=50 mA cm^{-2}, t_{on}=1 ms, t_{off}= 20 ms, T=348 K). The *lines* represent fits with the grain-growth model with size-dependent impediment. *Inset*: temperature dependence of the rate constants in extended Arrhenius representations. The resulting activation energy is 37 kJ mol^{-1}

constants resulting from the fits obeys the Arrhenius law (see inset in Fig. 5) and yields an activation of 37 kJ mol^{-1} for the grain growth of nanocrystalline gold. According to Landolt-Boernstein [26], in the temperature range of 640–717 K, the activation energy for grain boundary self-diffusion in microcrystalline gold has a value of 84.9 kJ mol^{-1}. The disagreement between our result and the literature value can be related to the difference in the grain boundary structure between nanocrystalline and coarse-grained materials and therefore to the difference in the mechanism of grain boundary self-diffusion.

Conclusions

A stable electrolyte with high effectiveness, free of cyanides and sulfites, has been prepared for gold electroplating. Nanoscaling has been achieved by pulsed current electrodeposition. The current density, pulse duration, bath temperature, and composition have been utilized for the variation of the crystallite size, as well as for controlling physical properties such as thermal stability. Sulfur- or arsenic-containing additives decrease the gold crystallite size in the electroplating process down to 7 nm and increase the thermal stability of gold samples up to 673 K. Gold alloys with copper, silver, palladium, and platinum could also be electrodeposited with crystallite sizes in the nanoscale range. The grain-growth kinetics of nanostructured gold has been evaluated in terms of a growth model with size-dependent impediment; the resulting activation energy of grain growth in nanocrystalline gold is considerably lower than the activation energy for grain boundary self-diffusion in coarse-grained gold.

Compared to chemical or physical methods, the electrochemical preparative and analytical procedures are cheap and versatile, and further investigations in this field are in progress now.

Acknowledgments The present work is initiated and performed at the Universität des Saarlandes (Germany) in the framework of the Sonderforschungsbereich 277 (Grenzflächenbestimmte Materialien). For experimental assistance, we thank S. Kuhn.

References

1. Popov KI, Pavlovic MG (1993) Mod Aspects Electrochem 24:299
2. Robertson A, Erb U, Palumbo G (1999) Nanostruct Mater 12:1035
3. Natter H, Hempelmann R (2003) Electrochim Acta 49:51
4. Dinan TE, Cheh HY (1992) J Electrochem Soc 139:2
5. Harman GG (1991) Reliability and yield problems of wire bonding in microelectronics. ISHM, Reston
6. http://www.palomartechnologies.com/resources/whitepapers/makingconnection.htm
7. Li YG, Lasia A (1997) J Electrochem Soc 144:6
8. Osaka T, Kodera A, Misato T, Homma T, Okinaka Y (1997) J Electrochem Soc 144:10
9. Green TA, Liew MJ, Roy S (2003) J Electrochem Soc 150:3
10. Simon F (2000) Galvanotechnik 54:10
11. Puippe JC, Leaman F (eds) (1986) Theory and practise of pulse plating, Amer Electroplaters Soc, Florida
12. Bockris JO'M, Razumney GA (1967) Fundamental aspects of electrocrystallization. Plenum, New York
13. Kashchiev D (2000) Nucleation basic theory with applications. Butterworth-Heinemann, Oxford
14. Budevski, Staikov G, Lorenz WJ (1996) Electrochemical phase formation and growth. VCH, Weinheim
15. Warren BE, Averbach LE (1950) J Appl Phys 21:536
16. Warren BE, Averbach LE (1952) J Appl Phys 23:497
17. Warren BE (1990) X-ray diffraction. Dover, New York
18. Natter H, Hempelmann R (1996) J Phys Chem 100:19525
19. Natter H, Schmelzer M, Loffler MS, Krill CE, Fitch A, Hempelmann R (2000) J Phys Chem 104:2467
20. Holleman-Wiberg (1985) Lehrbuch der Anorganischen Chemie. Walter de Gruyter, Berlin
21. Lin K, Weil R (1986) J Electrochem Soc 133:4
22. Shunk FA (1969) Constitution of binary alloys, second supplement. McGraw-Hill, New York
23. http://ecsmeet2.peerx-press.org/ms_files/ecsmeet2/2005/05/27/00009260/00/9260_0_art_file_0_1117206052.pdf
24. Carotenuto G, Nicolais L (2003) J Mater Chem 13
25. Michels A, Krill CE, Erhardt H, Birringer R, Wu DT (1999) Acta Mater 47:2143
26. Landolt-Boernstein (1990) Numerical data and functional relationships in science and technology. Springer, Berlin Heidelberg New York, p. 640